Mechanical Technology and Engineering Insights

www.mtei.reapress.com

Mech. Technol. Eng. Insights. Vol. 2, No. 2 (2025) 94–104.

Paper Type: Original Article

Numerical Investigation of Natural Convection Heat Transfer in Turbulent Flow Inside a Square Enclosure Using Large Eddy Simulation with the Lattice Boltzmann Method

Seyed Ahmad Edalatpanah[1,*], Hashem Saberi Najafi[2]

[1] Department of Industrial Engineering, Yonsei University, Seoul, South Korea; Department of Applied Mathematics, Graphic Era Hill University, Dehradun, India; s.a.edalatpanah@aihe.ac.ir.

[2] Department of Applied Mathematics and Computer Science, Faculty of Mathematical Sciences, University of Guilan, Rasht, Iran; hnajafi@guilan.ac.ir.

Citation:

Received: 10 October 2024 *Revised: 18 December 2024* *Accepted: 12 Februray 2025*	Edalatpanah, S. A., & Saberi Najafi, H. (2025). Numerical investigation of natural convection heat transfer in turbulent flow inside a square enclosure using large eddy simulation with the lattice Boltzmann method. *Mechanical technology and engineering insights*, *2*(2), 94-104.

Abstract

The present study focuses on the numerical analysis of turbulent natural convection within a square enclosure with differentially heated vertical walls, and this is achieved by employing a Large Eddy Simulation (LES) approach coupled with the Lattice Boltzmann Method (LBM). The lattice model used for this study is based on the D2Q9 lattice for both hydrodynamic and thermal fields, and buoyancy effects are modeled using the Boussinesq approximation. The results for this study are presented using contours of stream function, isotherms, and mean Nusselt number. At moderate values of Rayleigh number, i.e., for $Ra \leq 10^8$, the thermal field within the core of the square cavity is found to be almost uniform, and this shows that heat transfer is due to conduction. However, for $Ra = 10^9$, significant distortions and oscillations within the isothermal contours show that turbulent convection is established within the square cavity.

Keywords: Turbulent natural convection, Large Eddy simulation, Lattice Boltzmann method, Square cavity.

1 | Introduction

The description of turbulent flow is one of the major problems in engineering and theoretical fluid mechanics. In turbulent flows, motions with large and small scales of eddies and dissipative structures coexist.

Numerical analysis of turbulent flows has been conducted in many studies [1–3]. Various models have been developed to describe turbulent flows, and one of the most popular models is that of Large-Eddy Simulation (LES) [4], [5] The LES model is widely used in many fields, including the analysis of geophysical phenomena in the atmosphere and ocean, and is considered one of the fundamental models of turbulent flows in fluid

Corresponding Author: s.a.edalatpanah@aihe.ac.ir

https://doi.org/10.48313/mtei.v2i2.42

mechanics and physics [6–9]. However, the analysis of turbulent flows requires specific information that can be obtained by numerical analysis, which leads to the development of new algorithms and the use of parallel computing tools. The selection of an optimal numerical method that balances efficiency and accuracy is one of the obvious problems.

The Lattice Boltzmann Method (LBM) has gained great popularity over the last two decades. Apart from its simplicity and efficiency, it is used for simulating complex flow problems in different boundary conditions, such as multiphase and multicomponent flows, turbulent flows, and micro-scale flows [10–16], [17–19]. The LBM has shown its potential in simulating turbulent flows efficiently, and its application in computational fluid dynamics has some benefits compared with other methods for simulating turbulence flows [20–24]. Moreover, it has greater generality because of the advantageous balance between efficiency and accuracy.

Yu et al. [25] used multiple relaxation times in the lattice Boltzmann equation for simulating turbulence flows by the method of Large Eddy Simulation (LES) and showed that it is a suitable method for simulating turbulence flows. Fernandino et al. [26] performed LES for simulating turbulent open-channel flows by the LBM and found good agreement with experimental results qualitatively. Chen [27] presented a novel and simple LES model based on the LBM for simulating two-dimensional turbulence flows and showed its efficiency, stability, and simplicity in simulating two-dimensional turbulence flows.

Kareem et al. [28] in their research paper proposed an LBM-based framework with a scheme for the simulation of convergent homogeneous turbulent flows. The authors observed that the turbulence characteristics of the flow, regardless of the model used, are achieved by methods similar to those used in the simulation of the flow in previous investigations. In the study by Nee [29], the author presented the application of hybrid lattice Boltzmann models for simulating natural convection heat transfer up to Rayleigh numbers of 10^{12}. Yu et al. [25] presented the application of multiple relaxation times in the lattice Boltzmann equation for simulating LESs of turbulent flows and found it applicable for the simulation of such flows. Chen et al. [30] developed a new thermal lattice Boltzmann model for the simulation of natural convection in fluids with a high Prandtl number.

Chen [30] developed a simple and innovative LES model based on the LBM for the simulation of two-dimensional turbulent flows. The authors proved that the model is efficient, stable, and simple for the simulation of two-dimensional turbulence. Polasanapalli and Anupindi [31] developed a lattice Boltzmann-based solver for the simulation of turbulent natural convection in cylindrical cavities by the LES method. Moreover, Han et al. [32] performed a numerical analysis on the LES in the LBM for the simulation of airflow in a non-isothermal enclosed cavity. Agoujil et al. [33] simulated the process of natural convection with the LBM, considering a localized heating process within a cavity. Moreover, Lin et al. [34] derived a set of scaling laws for the boundary layer of a natural convection process, which can be employed for the validation of turbulence models.

The primary objective of this study is to introduce a turbulence model based on the LBM, considering a simple and explicit form. For this purpose, turbulent natural convection is simulated within a cavity, considering a wide range of Rayleigh numbers. Initially, a brief introduction is made about the LBM, followed by the application of LES within this method, and then the results are compared with those of earlier studies.

2|Geometry and Problem Description

The geometric configuration of interest is given in *Fig. 1* and consists of a two-dimensional square cavity of height H and width W, where H = W. The fluid inside is air with a Prandtl number of Pr = 0.71 and is considered a Newtonian fluid with constant properties, except for its density in the buoyancy term as given by the Boussinesq approximation.

The Mach number is set at Ma = 0.1 and is used to maintain an incompressible fluid flow regime in the implementation of the LBM. The fluid inside is air with Prandtl number Pr = 0.71, as is common in natural convection problems.

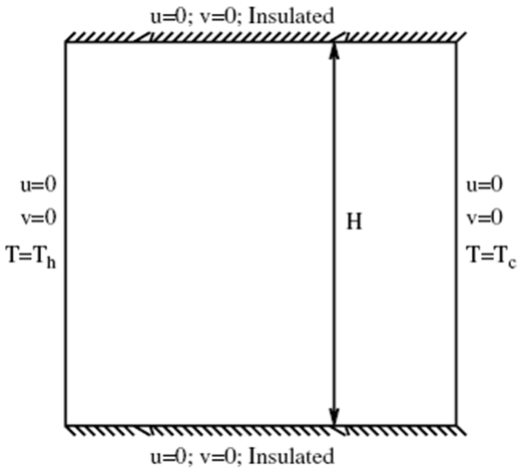

Fig. 1. Geometry of the problem.

3|Governing Equations

In the lattice Boltzmann model of incompressible thermal flows, two distribution functions, namely f and g, are used to describe the flow and temperature fields, respectively. These functions are used to compute the macroscopic flow variables, which include velocity, temperature, and pressure. An important characteristic of the LBM is that all parameters are made dimensionless. In this study, a square grid and the D2Q9 model, shown in *Fig. 2*, are used for both flow and temperature distribution functions.

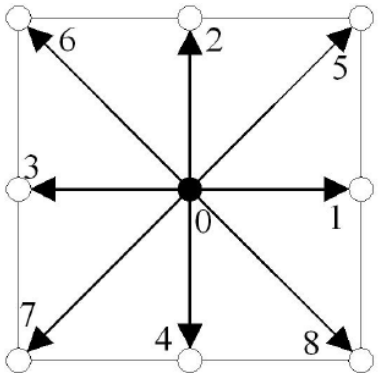

Fig. 2. D2Q9 model.

By discretizing the Navier-Stokes equations, the governing equations for the flow and temperature distribution functions are written as follows [25], [35-37]:

For the flow field:

$$f_i(x + c_i\Delta T, t + \Delta t) - f_i(x,t) = \frac{1}{\tau_v}\left[f_i(x,t) - f_i^{eq}(x,t)\right] + \Delta t c_i F \quad (1)$$

For the temperature field:

$$g_i\left(x + c_i\Delta T, t + \Delta t\right) - g_i(x,t) = \frac{1}{\tau_c}\left[g_i\left(x,t\right) - g_i^{eq}\left(x,t\right)\right] \quad (2)$$

In these relations, c_k is the discrete velocity vector, Δt is the time step, and τ_f and τ_g are the relaxation times for the flow and temperature fields, respectively. f_k^{eq} and g_k^{eq} are the local equilibrium distribution functions, which are calculated according to the following relations for the flow and temperature fields. Furthermore, F represents the external force.

$$f_i^{eq}(x,t) = \omega_i \rho \left[1 + \frac{c_i u}{c_s^2} + \frac{1}{2}\frac{(c_i u)^2}{c_s^4} - \frac{1}{2}\frac{u.u}{c_s^2} \right] \quad (3)$$

$$g_i^{eq} = \omega_i T \left[1 + \frac{c_i u}{c_s^2} \right] \quad (4)$$

The discrete velocity vector c_k for the D2Q9 model is defined as follows:

$$c_i = \begin{cases} 0 i = 0 \\ c\left(\cos\left[(i-1)\frac{\pi}{2}\right], \sin\left[(i-1)\frac{\pi}{2}\right]\right) i = 1-4 \\ c\sqrt{2}\left(\cos\left[(i-5)\frac{\pi}{2}+\frac{\pi}{4}\right], \sin\left[(i-5)\frac{\pi}{2}+\frac{\pi}{4}\right]\right) i = 5-8 \end{cases} \quad (5)$$

In these relations, $c = \Delta x/\Delta t = \Delta y/\Delta t$, where Δx and Δy are the grid spacings in the x and y directions. To improve numerical stability, T_m, the average temperature value, is used to calculate c_s. Using the Chapman-Enskog expansion, the Navier-Stokes equations can be recovered with the proposed model. The kinematic viscosity and thermal diffusion coefficient are related to the relaxation times as follows:

$$\vartheta = \left[\tau_\nu - \frac{1}{2}\right] c_s^2 \Delta t \alpha = \left[\tau_c - \frac{1}{2}\right] c_s^2 \Delta t \quad (6)$$

In these relations, c_s is the speed of sound and equals $c/\sqrt{3}$. In the present simulation, the Boussinesq approximation is used to model the buoyancy force. The external force F is defined as follows:

$$F_i = 3\omega_i g_y \beta \Delta T \quad (7)$$

In this relation, β is the thermal expansion coefficient, g_y is the gravitational acceleration, and ΔT is the temperature difference. Finally, the macroscopic quantities of density, velocity, and temperature are calculated using the following relations:

$$\rho = \sum_i f_i \quad (8)$$

$$\rho u_j = \sum_i f_i c_{ij} \quad (9)$$

$$T = \sum_i g_i \quad (10)$$

In the LES model, the main objective is to calculate the turbulent viscosity ν_t such that the total viscosity equals $\alpha_t = \frac{\nu_t}{pr_t}$ in this relation, Pr_t is the turbulent Prandtl number, which is considered to be 0.4. The relevant calculations are performed as follows:

$$\nu_t = (C\Delta)^2 \left(|\bar{S}|^2 + \frac{pr}{pr_t} \nabla T . \frac{\vec{g}}{|\vec{g}|} \right)^{1/2} \quad (11)$$

In this relation, C is the Smagorinsky constant, assumed to be 0.1. $\Delta = \sqrt{(\Delta x)^2 + (\Delta y)^2}$ is the filter width, and Δx and Δy are the grid spacings in the x and y directions. The term $|S|$ is defined as follows:

$$|\bar{S}| = \sqrt{2\bar{S}_{\alpha\beta}\bar{S}_{\alpha\beta}} \quad (12)$$

$$\bar{S}_{\alpha\beta} = \frac{(\partial_\alpha \bar{u}_\beta + \partial_\beta \bar{u}_\alpha)}{2} \quad (13)$$

3.1 | Lattice Boltzmann Method Based on the Large Eddy Simulation Model

Applying the LES model in the LBM is straightforward and is achieved by affecting the relaxation time [22–24]:

$$\nu_{totol} = c_s^2\left(\tau_\nu - 0.5\right) = \nu_0 + \nu_t \quad \textbf{(14)}$$

In this relation, ν_0 and ν_{totol} indicate the initial viscosity and the total viscosity, respectively:

$$\tau_\nu = \frac{\left(\nu_0 + \nu_t\right)}{c_s^2} + 0.5 = \frac{\nu_0}{c_s^2} + 0.5 + \frac{\nu_t}{c_s^2} = \tau_0 + \frac{\nu_t}{c_s^2} \quad \textbf{(15)}$$

The strain rate tensor in the LBM is calculated as follows:

$$\left|\bar{S}\right| = \frac{3}{2\tau_m}\left|Q\right| \quad \textbf{(15)}$$

$$Q = \sum_{i=0}^{8} e_{i\alpha} e_{i\beta}\left(f_i - f_i^{eq}\right) \quad \textbf{(16)}$$

By substituting $|S|$ into *Eq. (11)*, the turbulent viscosity is calculated, and then the total relaxation time for the flow field is obtained from the following relation:

$$\nu_t = \left(C\Delta\right)^2\left(\frac{9}{4\tau_m^2}\left|Q\right|^2 + \frac{pr}{pr_t}\nabla T.\frac{\vec{g}}{\left|\vec{g}\right|}\right)^{1/2} \quad \textbf{(17)}$$

The relaxation time for the temperature distribution functions is calculated similarly using the following relation:

$$\tau_c = \tau_{D0} + \frac{\alpha_t}{c_s^2} = \tau_{Do} + \frac{\frac{\nu_t}{pr_t}}{c_s^2} \quad \textbf{(18)}$$

By substituting the obtained relaxation times into *Eqs. (1)* and *(2)*, the LES model is applied within the LBM.

3.2 | Applying Boundary Conditions

Flow

The geometry of the problem is shown in *Fig. 1*, and the D2Q9 arrangement is shown in *Fig. 2*. Implementing boundary conditions is important for the simulation. Considering the no-slip condition, the bounce-back boundary condition is used for the solid boundaries. For example, the unknown density distribution functions on the right wall are determined using the following condition:

$$f_{6,n} = f_{8,n}f_{7,n} = f_{5,n}f_{3,n} = f_{1,n}, \quad \textbf{(19)}$$

where *n* represents the node on the boundary.

Temperature

The top and bottom walls of the cavity are insulated, and the bounce-back boundary condition is also used for them. The temperature on the left and right walls is specified: on the left wall, T_H=1.0, and on the right wall, T_C= 0. Due to the use of the D2Q9 model, the distribution functions g_1, g_5, and g_8 on the left wall are unknown and are calculated as follows:

$$g_1 = T_H\left(\omega_1 + \omega_3\right) - g_3 \quad \textbf{(20)}$$

$$g_5 = T_H(\omega_5 + \omega_7) - g_7 \quad (21)$$

$$g_8 = T_H(\omega_8 + \omega_6) - g_6 \quad (22)$$

And for the right wall, the unknown distribution functions are calculated as follows:

$$g_3 = T_c(\omega_1 + \omega_3) - g_1 \quad (23)$$

$$g_7 = T_c(\omega_5 - \omega_7) - g_5 \quad (24)$$

$$g_6 = T_c(\omega_8 + \omega_6) - g_8 \quad (25)$$

The Nusselt number is one of the most important dimensionless parameters in describing convective heat transfer. The local Nusselt number and its average values on the hot and cold walls were calculated as follows:

$$NU_y = -\frac{L}{\Delta T}\frac{\partial T}{\partial x} \quad (26)$$

$$NU_{avg} = \frac{1}{L}\int_0^L NU_y \, dy \quad (27)$$

4 | Validation of the Numerical Solution

Table 1 shows a comparison between the average Nusselt numbers for different Rayleigh numbers. It is evident that the results are in good agreement with previous studies.

Table 1. Comparison of the average Nusselt number with previous works.

Rayleigh Number (Ra)	Grid Resolution	Average Nusselt Number (Present Work)	Average Nusselt Number [19]	Average Nusselt Number [20]
1×10^6	128 × 128	8.78	8.80	8.65
1×10^7	128 × 128	16.51	—	16.80
1×10^8	512 × 512	30.71	32.20	30.50
1×10^9	512 × 512	59.10	60.10	57.40

4 | Results and Discussion

The results obtained are presented in this section. *Figs. 3* and *4* show the temperature contours and streamlines for Rayleigh numbers ranging from 10^6 to 10^9. The results obtained are in good agreement with the numerical analysis of turbulent flow within a cavity. The results clearly show the development of flow and thermal structures with increasing Rayleigh number.

For Ra = 10^6, the flow field is dominated by a single clockwise rotating cell that covers most of the enclosure. The contours of the stream function are smooth and well-organized, indicating a stable laminar flow field. As such, the isotherms are thicker and gently curved, indicating that heat transfer is dominated by conduction.

For Ra = 10^7, the buoyancy-induced flow field is much stronger than at Ra = 10^6. As such, the flow field has developed secondary vortical structures at the corners of the enclosure. The streamlines are compressed at the vertical walls of the enclosure, indicating higher velocity gradients at these walls. The isotherms are significantly distorted, especially at the hot and cold walls, indicating the development of thermal boundary layers and a transition towards convection-dominated heat transfer.

At Ra = 10^8, there is significant unsteadiness and complexity in the flow. There are multiple vortices and distorted streamline patterns, especially in the upper and lower areas of the cavity. The isotherms are nearly horizontal in the core region, indicating strong thermal mixing and a good stratification of the temperature field. The thermal boundary layers near the vertical walls are also reduced, suggesting that the heat transfer by convection is increased.

In the case of the highest Rayleigh number, i.e., Ra = 10^9, the flow field is complex and turbulent. There are multiple interacting vortices of different scales, especially in the upper part of the enclosure, according to the contours of the stream function. This suggests that there is significant buoyancy-driven instability in this flow field. The isotherms show significant distortion and clustering near the walls, while they remain nearly uniform in the core region. This suggests that convection is dominant over conduction, and there is a significant enhancement of heat transfer.

Thus, an increase in the value of the Rayleigh number causes a significant transition from laminar to turbulent natural convection with smaller thermal boundary layers, more complex flow structures, and an appreciable improvement in the performance of natural convection. The above results are in accordance with the numerical and experimental studies of turbulent natural convection in closed enclosures.

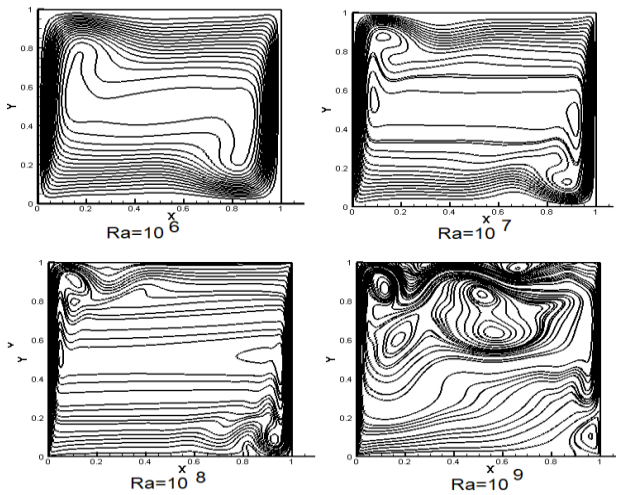

Fig. 3. The streamlines for Rayleigh numbers ranging from 10^6 to 10^9.

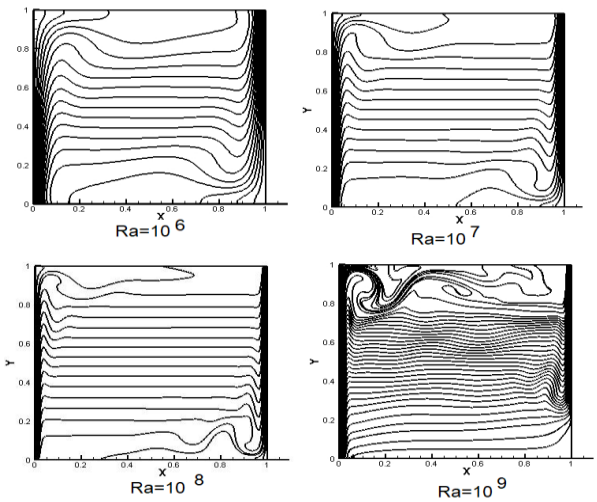

Fig. 4. The temperature contours for Rayleigh numbers ranging from 10^6 to 10^9.

Furthermore, Variation of the dimensionless temperature along the horizontal direction for three different values of the Rayleigh number is shown in *Fig. 5*. It is clear that near the vertical walls on the left and right sides, there are significant temperature gradients, which confirm the presence of boundary layers. Also, with an increase in the value of the Rayleigh number, the boundary layer thickness decreases, showing an improvement in the rate of convective heat transfer.

In the central region of the enclosure, the temperature profile seems almost uniform for all values of the Rayleigh number, which confirms the well-mixed thermal field due to the presence of a strong convective heat transfer mechanism. However, with an increase in the value of the Rayleigh number, the dimensionless temperature in the central region of the enclosure decreases, which might be due to the improvement in the mixing of fluids due to an increase in the value of the Rayleigh number. From the above results, it might be concluded that with an increase in the value of the Rayleigh number, the rate of convective heat transfer improves, showing sharper temperature gradients near the vertical walls and a uniform temperature profile in the central region of the enclosure.

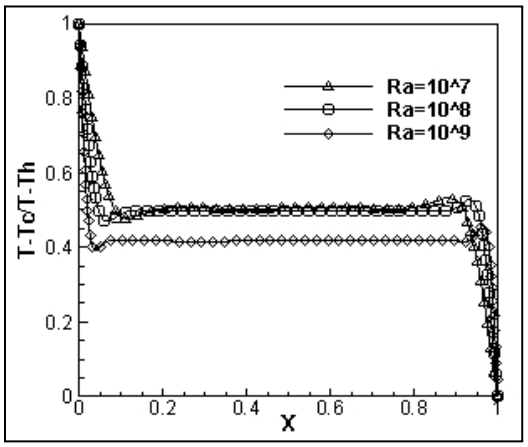

Fig. 5. The dimensionless temperature along the horizontal direction for three different values of the Rayleigh number.

5 | Conclusion

The numerical analysis of turbulent natural convection within a square enclosure subjected to differentially heated vertical walls has been carried out using the LES model and the LBM. The analysis was performed by considering different Rayleigh numbers from 10^6 to 10^9. The numerical results show that the buoyancy-induced flow increases with the increase of the Rayleigh number, resulting in the reduction of the thermal boundary layers and the development of more complex flow structures. The heat transfer within the core of the enclosure is found to be mainly conductive at lower Rayleigh numbers, whereas the role of the convective mechanism increases as the Rayleigh numbers increase. At Ra = 10^9, the flow structure shows characteristics of turbulent flow, including distorted isotherms and the presence of multiple, interacting vortices. The uniformity of the temperature field increases within the core of the enclosure as the Rayleigh numbers increase, which indicates the enhancement of the heat transfer due to the turbulent flow. The numerical results show good agreement with the benchmark solutions, which indicates the accuracy and reliability of the LES-LBM method.

Conflict of Interest

The authors declare no conflict of interest.

Data Availability

All data are included in the text.

Funding

This research received no specific grant from funding agencies in the public, commercial, or not-for-profit sectors.

Reference

[1] Markatos, N. C., & Pericleous, K. A. (1984). Laminar and turbulent natural convection in an enclosed cavity. *International journal of heat and mass transfer*, *27*(5), 755–772. https://doi.org/10.1016/0017-9310(84)90145-5

[2] Le Quéré, P. (1991). Accurate solutions to the square thermally driven cavity at high Rayleigh number. *Computers & fluids*, *20*(1), 29–41. https://doi.org/10.1016/0045-7930(91)90025-D

[3] Henkes, R., & Hoogendoorn, C. J. (1993). Scaling of the laminar natural-convection flow in a heated square cavity. *International journal of heat and mass transfer*, *36*(11), 2913–2925. https://doi.org/10.1016/0017-9310(93)90110-R

[4] Milane, R. E. (2004). Large eddy simulation (2D) using diffusion--velocity method and vortex-in-cell. *International journal for numerical methods in fluids*, *44*(8), 837–860. https://doi.org/10.1002/fld.673

[5] Kraichnan, R. H., & Montgomery, D. (1980). Two-dimensional turbulence. *Reports on progress in physics*, *43*(5), 547–619. https://doi.org/10.1088/0034-4885/43/5/001

[6] Ganji, D. D. (2006). The application of He's homotopy perturbation method to nonlinear equations arising in heat transfer. *Physics letters a*, *355*(4–5), 337–341. https://doi.org/10.1016/j.physleta.2006.02.056

[7] Jalaal, M., & Ganji, D. D. (2011). On unsteady rolling motion of spheres in inclined tubes filled with incompressible Newtonian fluids. *Advanced powder technology*, *22*(1), 58–67. https://doi.org/10.1016/j.apt.2010.03.011

[8] Jalaal, M., & Ganji, D. D. (2010). An analytical study on motion of a sphere rolling down an inclined plane submerged in a Newtonian fluid. *Powder technology*, *198*(1), 82–92. https://doi.org/10.1016/j.powtec.2009.10.018

[9] Jalaal, M., Ganji, D. D., & Ahmadi, G. (2010). Analytical investigation on acceleration motion of a vertically falling spherical particle in incompressible Newtonian media. *Advanced powder technology*, *21*(3), 298–304. https://doi.org/10.1016/j.apt.2009.12.010

[10] Aidun, C. K., & Clausen, J. R. (2010). Lattice-Boltzmann method for complex flows. *Annual review of fluid mechanics*, *42*(1), 439–472. https://doi.org/10.1146/annurev-fluid-121108-145519

[11] Ampofo, F., & Karayiannis, T. G. (2003). Experimental benchmark data for turbulent natural convection in an air filled square cavity. *International journal of heat and mass transfer*, *46*(19), 3551–3572. https://doi.org/10.1016/S0017-9310(03)00147-9

[12] Chen, H., Kandasamy, S., Orszag, S., Shock, R., Succi, S., & Yakhot, V. (2003). Extended Boltzmann kinetic equation for turbulent flows. *Science*, *301*(5633), 633–636. https://doi.org/10.1126/science.1085048

[13] Yu, D., Mei, R., Luo, L. S., & Shyy, W. (2003). Viscous flow computations with the method of lattice Boltzmann equation. *Progress in aerospace sciences*, *39*(5), 329–367. https://doi.org/10.1016/S0376-0421(03)00003-4

[14] Chakraborty, S., & Chatterjee, D. (2007). An enthalpy-based hybrid lattice-Boltzmann method for modelling solid--liquid phase transition in the presence of convective transport. *Journal of fluid mechanics*, *592*, 155–175. https://doi.org/10.1017/S0022112007008555

[15] Guo, Z., Zheng, C., & Shi, B. (2008). Lattice Boltzmann equation with multiple effective relaxation times for gaseous microscale flow. *Physical review e—statistical, nonlinear, and soft matter physics*, *77*(3), 36707. https://doi.org/10.1103/PhysRevE.77.036707

[16] Raabe, D. (2004). Overview of the lattice Boltzmann method for nano-and microscale fluid dynamics in materials science and engineering. *Modelling and simulation in materials science and engineering*, *12*(6), R13--R46. https://doi.org/10.1088/0965-0393/12/6/R01

[17] Meng, J., Qian, Y., Li, X., & Dai, S. (2008). Lattice Boltzmann model for traffic flow. *Physical review e—statistical, nonlinear, and soft matter physics*, *77*(3), 36108. https://doi.org/10.1103/PhysRevE.77.036108

[18] Furtado, K., & Yeomans, J. M. (2006). Lattice Boltzmann simulations of phase separation in chemically reactive binary fluids. *Physical review e—statistical, nonlinear, and soft matter physics*, *73*(6), 66124. https://doi.org/10.1103/PhysRevE.73.066124

[19] Barakos, G., Mitsoulis, E., & Assimacopoulos, D. O. (1994). Natural convection flow in a square cavity revisited: Laminar and turbulent models with wall functions. *International journal for numerical methods in fluids*, *18*(7), 695–719. https://doi.org/10.1002/fld.1650180705

[20] Dixit, H. N., & Babu, V. (2006). Simulation of high Rayleigh number natural convection in a square cavity using the lattice Boltzmann method. *International journal of heat and mass transfer*, *49*(3–4), 727–739. https://doi.org/10.1016/j.ijheatmasstransfer.2005.07.046

[21] Horvat, A., Kljenak, I., & Marn, J. (2001). Two-dimensional large-eddy simulation of turbulent natural convection due to internal heat generation. *International journal of heat and mass transfer*, *44*(21), 3985–3995. https://doi.org/10.1016/S0017-9310(01)00066-7

[22] Hou, S., Sterling, J., Chen, S., & Doolen, G. (1996). A Lattice Boltzmann Subgrid Model for High Reynolds. *Pattern formation and lattice gas automata, american mathematical soc*, *6*(6), 151. https://archive.org/details/arxiv-comp-gas9401004

[23] Teixeira, C. M. (1998). Incorporating turbulence models into the lattice-Boltzmann method. *International journal of modern physics c*, *9*(08), 1159–1175. https://doi.org/10.1142/S0129183198001060

[24] Krafczyk, M., Tölke, J., & Luo, L. S. (2003). Large-eddy simulations with a multiple-relaxation-time LBE model. *International journal of modern physics b*, *17*(01n02), 33–39. https://ui.adsabs.harvard.edu/abs/2003IJMPB..17...33K/abstract

[25] Yu, H., Luo, L. S., & Girimaji, S. S. (2006). LES of turbulent square jet flow using an MRT lattice Boltzmann model. *Computers & fluids*, *35*(8–9), 957–965. https://doi.org/10.1016/j.compfluid.2005.04.009

[26] Fernandino, M., Beronov, K., & Ytrehus, T. (2009). Large eddy simulation of turbulent open duct flow using a lattice Boltzmann approach. *Mathematics and computers in simulation*, *79*(5), 1520–1526. https://doi.org/10.1016/j.matcom.2008.07.001

[27] Chen, S. (2009). A large-eddy-based lattice Boltzmann model for turbulent flow simulation. *Applied mathematics and computation*, *215*(2), 591–598. https://doi.org/10.1016/j.amc.2009.05.040

[28] Kareem, W. A., Izawa, S., Xiong, A. K., & Fukunishi, Y. (2009). Lattice Boltzmann simulations of homogeneous isotropic turbulence. *Computers & mathematics with applications*, *58*(5), 1055–1061. https://doi.org/10.1016/j.camwa.2009.02.002

[29] Nee, A. (2025). Evaluation of hybrid lattice Boltzmann models for laminar and turbulent natural convection. *International communications in heat and mass transfer*, *162*, 108635. https://doi.org/10.1016/j.icheatmasstransfer.2025.108635

[30] Chen, S., Luo, K. H., Jain, A. K., Singh, D., & McGlinchey, D. (2023). Natural convection of large Prandtl number fluids: A controversy answered by a new thermal lattice Boltzmann model. *Case studies in thermal engineering*, *44*, 102827. https://doi.org/10.1016/j.csite.2023.102827

[31] Polasanapalli, S. R. G., & Anupindi, K. (2022). Large-eddy simulation of turbulent natural convection in a cylindrical cavity using an off-lattice Boltzmann method. *Physics of fluids*, *34*(3). https://doi.org/10.1063/5.0084515

[32] Han, M., Kikumoto, H., & Ooka, R. (2024). Numerical investigation of lattice Boltzmann method-based large-eddy simulation in non-isothermal enclosed cavity airflow. *International communications in heat and mass transfer*, *157*, 107698. https://doi.org/10.1016/j.icheatmasstransfer.2024.107698

[33] Agoujil, F., Elguennouni, Y., Ighris, Y., Baliti, J., & Hssikou, M. (2023). Modeling of natural convection by lattice boltzmann in a partially heated cavity. *E3S web of conferences* (Vol. 469, p. 71). EDP Sciences. https://doi.org/10.1051/e3sconf/202346900071

[34] Lin, W., Armfield, S. W., & Khatamifar, M. (2024). Scaling laws for natural convection boundary layer of a Pr> 1 fluid on a vertical solid surface subject to a sinusoidal temperature in a linearly-stratified ambient fluid. *Physics of fluids*, *36*(1). https://doi.org/10.1063/5.0191550

[35] Kefayati, G. H. R., Hosseinizadeh, S. F., Gorji, M., & Sajjadi, H. (2011). Lattice Boltzmann simulation of natural convection in tall enclosures using water/SiO2 nanofluid. *International communications in heat and mass transfer*, *38*(6), 798–805. https://doi.org/10.1016/j.icheatmasstransfer.2011.03.005

[36] Sajjadi, H., Gorji, M., Kefayati, G. H. R., Ganji, D. D., & Shayannia, M. (2011). Simulation of natural convection flow in an inclined open cavity using Lattice Boltzmann Method. *World academy of science,*

engineering and technology, *55*, 271–625. https://researchnow.flinders.edu.au/en/publications/simulation-of-natural-convection-flow-in-an-inclined-open-cavity-/

[37] Mussa, M. A., Abdullah, S., Azwadi, C. S. N., & Muhamad, N. (2011). Simulation of natural convection heat transfer in an enclosure by the lattice-Boltzmann method. *Computers & fluids*, *44*(1), 162–168. https://doi.org/10.1016/j.compfluid.2010.12.033